



Cytocompatibility Assessment of Si, Plasma Enhanced Chemical Vapor Deposition-Formed SiO₂ and Si₃N₄ Used for Neural Prosthesis: A Comparative Study

Tao Sun^{1,*}, Woo-Tae Park^{1,2}, John Wei Mong Tsang¹, Tack Boon Yee¹, and Minkyu Je¹

¹*Institute of Microelectronics, Agency for Science and Technology Research (A*STAR), Singapore*

²*Department of Mechanical and Automotive Engineering, Seoul National University of Science and Technology, Seoul, Republic of Korea*

SiO₂ and Si₃N₄ layers to be used in the microfabrication of a neural probe were formed on Si substrate through plasma enhanced chemical vapor deposition (PECVD). To ensure their cytocompatibility, the surface properties and cytocompatibility of the PECVD-formed SiO₂ and Si₃N₄ were investigated and compared. SEM images showed the SiO₂ and Si₃N₄ layers consisted of nano-sized particles. In accordance with water contact angle measurement, the surface of both PECVD-formed SiO₂ and Si₃N₄ layers were hydrophilic and there was no significant difference in wettability between them. A breast cancer cell line (MCF-7) was seeded on their surface to evaluate the cytocompatibility. After 3 days of cell culture, the adherent cells on PECVD-formed Si₃N₄ surface did not spread as well as those on Si or PECVD-formed SiO₂, and the cells on the surface of PECVD-formed SiO₂ and Si₃N₄ were significantly less than on Si. At day 7, however, there was no significant difference between them, in terms of cell morphology and number. Therefore, the PECVD-formed SiO₂ and Si₃N₄ layers did not exhibit acute cytotoxicity and were as cytocompatible as tissue culture polystyrene.

Keywords: BioMEMS, Plasma Enhanced Chemical Vapor Deposition, SiO₂, Si₃N₄, Cytocompatibility.

Neuroprosthetics is an emerging research field with the aim of restoring the damaged hearing, visual or motor functions.^{1,2} Recent advances in biological microelectromechanical Systems (BioMEMS) make it possible to develop microfabricated multichannel 3D neural probe array which can record extracellular neuronal activity with high spatial resolution and low noise-to-signal ratio.^{3,4} However, the reactive host tissue responses give rise to an imminent obstacle for the widespread clinical application of the neural prostheses. As a result of foreign body responses, fibrous tissue sheath forms around the neural probe to degrade the quality of neuronal signal.⁵ Nicolelis et al. reported that 40% of functional electrodes failed within the first 18 months.⁶ A recent clinical study for a tetraplegic human to restore lost motor functions via a pilot neuromotor prosthesis found abrupt signal loss at most electrodes after 11 months implantation.⁷ For the stability of tissue-probe interface, it is crucial to selecting biocompatible materials to fabricate the neural probe, designing

the geometry and dimension of the probe to reduce tissue damage, and integrating the drug release system into the probe to minimize the host tissue responses.

As SiO₂ and Si₃N₄ are typically dielectric materials for insulating conductor trace lines or packaging microelectronic devices, they are involved in our microfabrication processes to develop a novel porous Si neural probe with adaptive stiffness. Due to its high deposition rate, good adhesion and low pinhole density, plasma enhanced chemical vapor deposition (PECVD) is widely employed in the fabrication of MEMS and optoelectronic devices. More importantly, its low processing temperature (250~350 °C) not only makes PECVD attractive for the fabrication of temperature sensitive devices, but also allow large area thin film deposition on flexible polymeric substrates. In our probe microfabrication processes, PECVD technique is used to prepare the SiO₂ or Si₃N₄ insulating layer. Since the encapsulating layers of the device directly contact with the cortical tissue, the surface properties and biocompatibility of the PECVD-formed SiO₂ and Si₃N₄ play a vital role in the host tissue response to the neural probe.

*Author to whom correspondence should be addressed.

Although it was believed that SiO₂ and Si₃N₄ synthesized by other methods were biocompatible *in vitro* and *in vivo*, slight differences in fabrication methods, chemical and phase compositions can influence the results of biological assay. Hence, the results of the biocompatibility tests for these fabrication methods may not apply to the materials fabricated using PECVD technique. Moreover, the cytocompatibility for the PECVD-formed SiO₂ and Si₃N₄ layers has not been extensively studied and compared. In the current study, as a good first step toward ensuring the long-term biocompatibility of the neural probe, surface properties and cytocompatibility of the PECVD-formed SiO₂ and Si₃N₄ layers were investigated and compared. In addition, the resulting data from the current research can be used by BioMEMS device designers to guide non-conducting structural material selection.

8-inch *p*-type Si wafers with (100) crystal orientation were obtained from Sumco (Sumco Corp. Japan), and then standard piranha clean procedure was carried out to remove the contamination. Si samples were prepared by dicing the cleaned wafer into plates (5 mm × 5 mm). For SiO₂ samples, PECVD (Plasma-Therm 790, USA) was used to coat a 2 μm-thick SiO₂ layer on the cleaned wafer at a temperature of 250 °C and a pressure of 1200 mTorr. Similarly, a layer of Si₃N₄ (2 μm) was synthesized on the cleaned wafer via PECVD at a temperature of 250 °C and a pressure of 1600 mTorr. Finally, the SiO₂ and Si₃N₄ coated wafers were cut into the plates with the same dimension as the Si sample.

Field emission scanning electron microscopy (FE-SEM, JSM-6700F, JEOL, USA) was used to examine the surface morphology of Si, SiO₂, and Si₃N₄ samples. Wettability of samples was determined at room temperature by the sessile drop method using a contact angle goniometer.⁸

As a first step to evaluate biocompatibility, a breast cancer cell line (MCF-7, ATCC HTB-22) was used in this investigation in that it was known as a well-established model to assess cytotoxicity.^{9,10} Before seeding with MCF-7 cells, all samples were rinsed in 70% ethanol for 1 h and then exposed under ultraviolet (UV) light for 1 h. Subsequently, MCF-7 cells were seeded at 2.0 × 10⁵ cells/well onto tissue culture polystyrene (TCP, as the control), Si, SiO₂, and Si₃N₄, respectively.

Live/dead cell staining (live/dead viability/cytotoxicity kit, Invitrogen Co., USA) was performed to determine the viable and non-viable MCF-7 cells on the surface of Si, SiO₂ and Si₃N₄ samples at 1, 3, and 7 days of culture.¹¹ Living cells were stained in green with calcein-AM (excitation/emission, ~495 nm/~515 nm), and dead cells were stained red with EthD-1 (excitation/emission, ~495 nm/~635 nm). MCF-7 cells stained in green and red were visualized using a fluorescence microscope (Olympus BX61, Olympus Optical Co., Japan). Cell viability was calculated by counting the number of live cells as well as dead cells and then dividing the number of live

cells by the number of total cells. At least 7 areas were randomly chosen for the cell viability assessment.

The 3-(4,5-dimethylthiazol-2-yl)-2,5-diphenyltetrazolium bromide (MTT) assay was carried out to evaluate the cytotoxicity of Si, SiO₂ and Si₃N₄ samples.^{12,13} After 2, 3, 5 and 7 days of cell culture, 20 μL of MTT solution was added into each well and then the 48-well cell culture plate containing samples was incubated in a humidified atmosphere with 5% CO₂ at 37 °C for 4 hours. Subsequently, 100 μL dimethyl sulfoxide (DMSO) was added into each well to dissolve the formazan as a resolvent. Finally, the absorbance was recorded using a microplate reader (DTX 800 Series Multimode Detectors, Beckman Coulter, USA) at 570 nm wavelength, with a reference wavelength of 640 nm to evaluate the proliferation of MCF-7 cells on samples in comparison to the control.

Results are expressed as means ± standard deviation and statistical analyses between multiple groups were carried

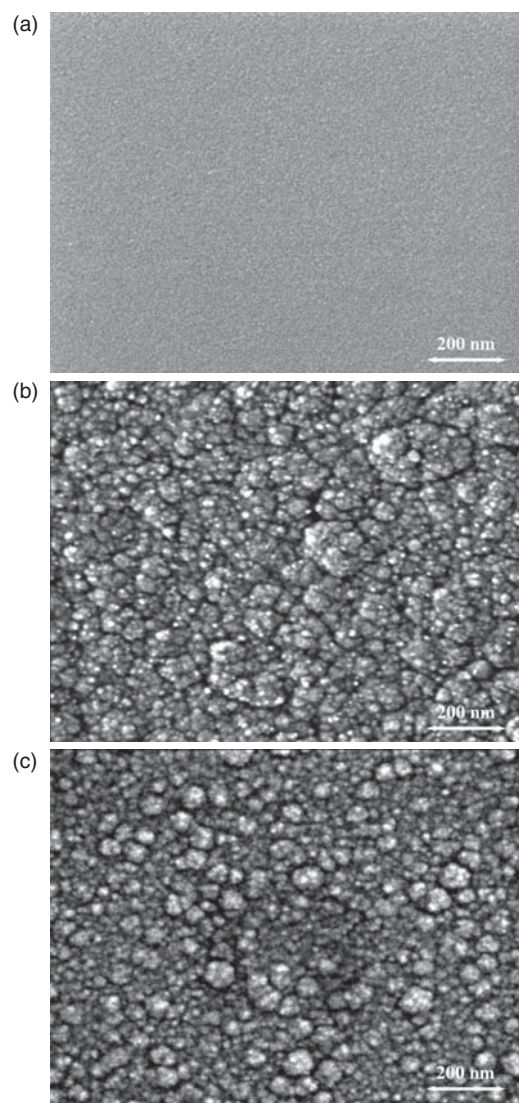


Fig. 1. Surface morphology of (a) Si, (b) SiO₂, and (c) Si₃N₄.

out using a one-way analysis of variance (ANOVA). Post hoc pairwise comparisons between individual groups were conducted using Tukey's test. *P* value less than 0.01 is considered statistically significant.

SEM surface morphology of samples is shown in Figure 1. The surface of Si samples was smooth and uniform, while the surface of SiO₂ and Si₃N₄ samples became rougher due to the formation of the layer consisting of nano-sized particles. Furthermore, no pinhole, peeling, cracking or other defects was found in the SEM images for the PECVD-formed SiO₂ and Si₃N₄ layers.

Figure 2 shows the water contact angles of Si, SiO₂ and Si₃N₄ samples. The water contact angle of Si ($48.5 \pm 3.6^\circ$) is significantly larger than either of other groups (*P* < 0.01). But there is no significant difference in water contact angle between SiO₂ and Si₃N₄ samples (*P* > 0.01). Kwon et al. suggested that the water contact angle of *p*-type Si (100) substrate was 51° , which was consistent with our results.¹⁴ Depending on surface roughness, the density of -OH functional group or fabrication methods, the water contact angle of PECVD SiO₂ varied from 20° to 65° .^{15,16} Similarly, the surface of Si₃N₄ was thought to be hydrophilic.¹⁷ Surface wettability is one of critical parameters determining the biological responses to an implanted material. It was known that artificial materials presenting moderate wettability with water contact angle of $40\sim 70^\circ$ effectively facilitated cell attachment.¹⁸ Therefore, the surface of the PECVD-formed SiO₂ and Si₃N₄ was supposed to be suitable for cell attachment.

As shown in Figure 3, morphology, proliferation and viability of MCF-7 cells seeded on Si, SiO₂ and Si₃N₄ were evaluated through live/dead staining. After 1 day of cell culture, most of cells on samples remained small and nearly spherical shapes and only a few spread cells with irregular protrusions were visualized on Si and SiO₂, indicating that at day 1 post-seeding most of cells on samples did not spread after initial attachment. At day 3 of cell culture, more cells were present on the surface of all samples, revealing that the adherent cells started to proliferate. In comparison with those on Si₃N₄, most of cells on Si and SiO₂ presented a larger size and spread extensively in all directions to form a polygonal configuration or spindle-like morphology. At day 7, the number of live cells on samples dramatically increased and a confluent cell layer was formed on the surface of all samples. Generally, cellular confluence is regarded as a natural process and phenomenon to describe the end point of cell proliferation. At this time point, there is no obvious difference in cell morphology between samples. Due to the almost negligible number of dead cells, the cell viability assessed by counting cells from randomly chose areas was over 99% for all samples at each time point.

Figure 4 illustrates the proliferation of MCF-7 cells on the TCP (control), Si, PECVD-formed SiO₂ and Si₃N₄ samples. In the MTT assay, the number of live cells on the surface of sample is directly proportional to the absorbance value. The absorbance of samples rose from day 2 to day 5, revealing that the cell number on the surface of samples

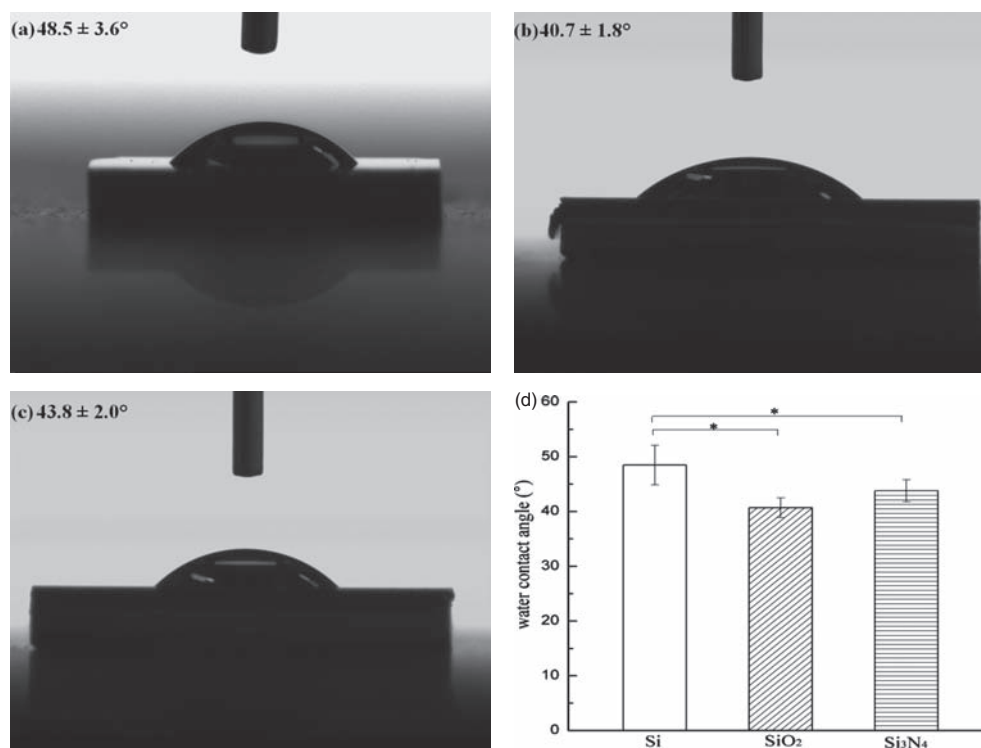


Fig. 2. Water contact angles of (a) Si, (b) SiO₂, (c) Si₃N₄, and (d) their statistical analysis. The statistical significance is indicated by * (*P* < 0.01).

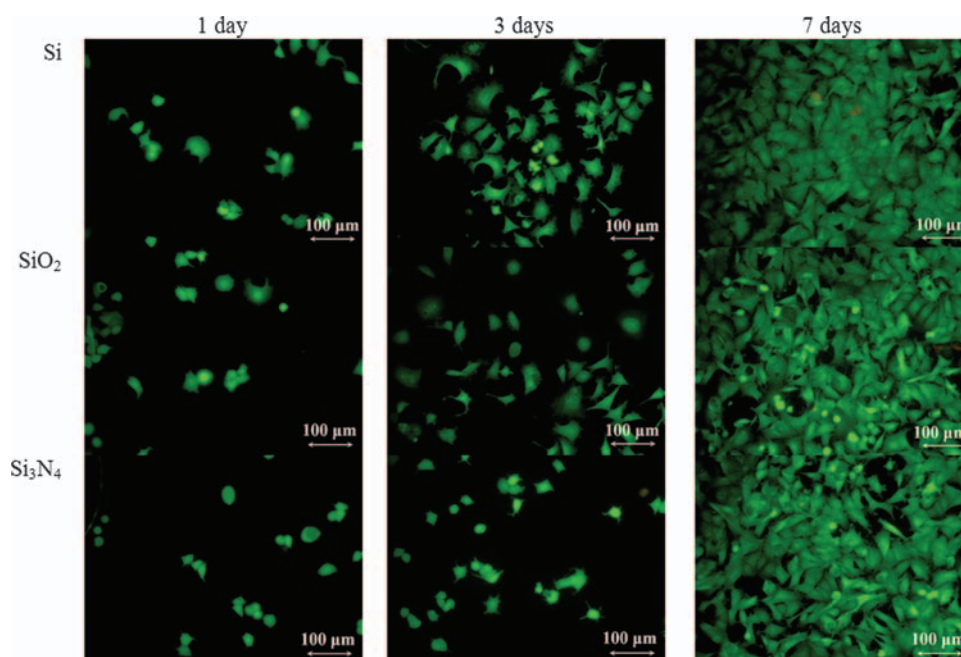


Fig. 3. Live/dead staining for MCF-7 cells on Si, SiO₂ and Si₃N₄ samples after 1 day, 3 days, and 7 days.

increased due to cell proliferation (Fig. 3). At day 7, however, the absorbance of samples did not continuously raise as before, because cells had grown into confluence (Figure 3) and reached the end point of cell proliferation. The absorbance of PECVD-formed Si₃N₄ samples was remarkably lower than that of TCP at day 2 ($P < 0.01$), and there was no significant difference among TCP, Si and PECVD-formed SiO₂ samples ($P > 0.01$). In addition, at day 3 MCF-7 cells on either SiO₂ or Si₃N₄ surface was significantly less than those on Si surface. However, there was no significant difference in absorbance between various types of samples after 5 and 7 days of culture ($P > 0.01$), suggesting that Si, PECVD-formed SiO₂ and Si₃N₄ did not exhibit the acute cytotoxicity and were as cytocompatible as TCP.

Cell attachment and proliferation can be influenced by physical and chemical properties of substrates, such as wettability, surface roughness, electrical charge, topography, or the presence of carbon, amine or oxygen groups. For example, it was reported that the NH₂ groups resulting from the precursor gases (SiH₄, NH₃ and N₂) on the surface of Si₃N₄ might improve the cell attachment.¹⁹ Additionally, after 7 days of culture rat calvarial osteoblasts showed a significantly increased proliferation with increasing surface roughness value R_a from 1.12 to 5.70 μm . However, the opposite proliferation behavior occurred for human gingival fibroblasts.²⁰ In the current research, the surface of the PECVD-formed SiO₂ and Si possessed nano-scale features which might provide more sites for cell attachment. But no enhanced cell attachment or proliferation on the surface of the PECVD-formed SiO₂ or Si₃N₄ was detected. Other studies suggested that no effect of nanoscale roughness on proliferation in absence of

microscale surface roughness.^{21,22} Gittens et al. believed that osteoblast proliferation and differentiation could be improved by combining the nanoscale structures with micro-/submicro-scale roughness.²³

On the basis of results from the current research, there is no significant difference between the PECVD-formed SiO₂ and Si₃N₄ to be used in the neural probe micro-fabrication, in terms of wettability and acute cytotoxicity. In order to select proper insulating materials for BioMEMS devices, other properties, such as mechanical properties, water permeability, antibiofouling ability, etc., should be considered and further investigated for the PECVD-formed SiO₂ and Si₃N₄ due to chemically aggressive physiological environment.

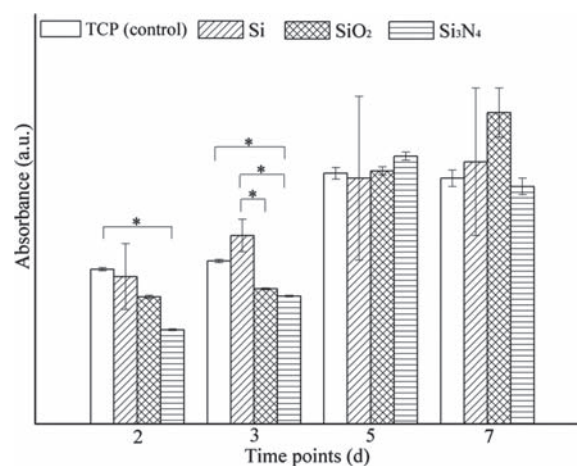


Fig. 4. Proliferation of MCF-7 cells on the control (TCP), Si, SiO₂, and Si₃N₄ samples as a function of cell culture time. The statistical significance is indicated by * ($P < 0.01$).

1. CONCLUSIONS

SiO₂ and Si₃N₄ layers were prepared on Si substrate for the fabrication of a neural probe, using PECVD technique. SEM observation showed that both of PECVD-formed SiO₂ and Si₃N₄ layers were composed of nano-sized particles and no thin film defects were found. Water contact angles of the PECVD-formed SiO₂ and Si₃N₄ were $40.7 \pm 1.8^\circ$ and $43.8 \pm 2^\circ$, respectively ($P > 0.01$). At day 3 of cell culture, MCF-7 cells on SiO₂ or Si₃N₄ surface were significantly less than those on Si ($P < 0.01$). Moreover, most of cells on Si₃N₄ surface did not spread extensively as those on Si or SiO₂ surface. However, a confluent cell layer was formed on the surface of all samples at day 7, and there was no significant difference in cell morphology or proliferation among all samples. Furthermore, at each time point the cell viability of the PECVD-formed SiO₂ and Si₃N₄ were more than 99% and the dead cells on their surface could be neglected. Hence, PECVD-formed SiO₂ and Si₃N₄ did not possess the acute cytotoxicity and were as cytocompatible as TCP.

Acknowledgments: This work was supported by the Science and Engineering Research Council of Agency for Science, Technology and Research (A*STAR) under Grant 1021710159. The authors thank staffs in the Bioelectronics Lab, Institute of Microelectronics for their generous help and valuable suggestions.

References and Notes

1. E. M. Maynard, *Annu. Rev. Biomed. Eng.* 3, 145 (2001).
2. H. Scherberger, *Curr. Opin. Neurobiol.* 19, 629 (2009).
3. S. Herwik, S. Kisban, A. A. A. Aarts, K. Seidl, G. Girardeau, K. Benchenane, M. B. Zugaro, S. I. Wiener, O. Paul, H. P. Neves, and P. Ruther, *J. Micromech. Microeng.* 19, 074008 (2009).
4. T. Sun, W. T. Park, M. Y. Cheng, J. Z. An, R. F. Xue, K. L. Tan, and M. Je, *IEEE Trans. Biomed. Eng.* 59, 390 (2012).
5. V. S. Polikov, P. A. Tresco, and W. M. Reichert, *J. Neurosci. Methods* 148, 1 (2005).
6. M. A. L. Nicolelis, D. Dimitrov, J. M. Carmena, R. Crist, G. Lehew, J. D. Kralik, and S. P. Wise, *Proc. Natl. Acad. Sci. USA* 100, 11041 (2003).
7. L. R. Hocherg, M. D. Serruya, G. M. Friebs, J. A. Mukand, M. Saleh, A. H. Caplan, A. Branner, D. Chen, R. D. Penn, and J. P. Donoghue, *Nature* 442, 164 (2006).
8. N. Gupta, S. Sasikala, and H. C. Barshilia, *Nanosci. Nanotech. Lett.* 4, 757 (2012).
9. T. Sun, L. P. Wang, M. Wang, H. W. Tong, and W. W. Lu, *Mater. Sci. Eng. C* 32, 1469 (2012).
10. T. Sun, N. Y. Zheng, and M. Wang, *Int. J. Appl. Ceram. Technol.* 9, 517 (2012).
11. T. Sun, M. Wang, and W. C. Lee, *Mater. Chem. Phys.* 130, 45 (2011).
12. A. V. Liopo, A. Conjusteau, O. V. Chumakova, S. A. Ermilov, R. Su, and A. A. Oreavsky, *Nanosci. Nanotech. Lett.* 4, 879 (2012).
13. T. Sun, L. P. Wang, M. Wang, H. W. Tong, and W. W. Lu, *Thin Solid Films* 519, 4623 (2011).
14. Y. B. Kwon, B. M. Weon, K. H. Won, J. H. Je, Y. Hwu, and G. Margaritondo, *Langmuir* 25, 1927 (2009).
15. F. Zhang, G. Baralia, A. Boborodea, C. Bailly, B. Nysten, and A. M. Jonas, *Langmuir* 21, 7427 (2005).
16. R. P. Gandhiraman, S. Daniels, and D. C. Cameron, *Plasma Process Polym.* 4, S369 (2007).
17. G. J. Wan, P. Yang, X. J. Shi, M. Wong, H. F. Zhou, N. Huang, and P. K. Chu, *Surf. Coat. Technol.* 200, 1945 (2005).
18. Y. Arima and H. Iwata, *Biomaterials* 28, 3074 (2007).
19. J. Wei, P. L. Ong, F. E. H. Tay, and C. Iliescu, *Thin Solid Films* 516, 5181 (2008).
20. T. P. Kunzler, T. Drobek, M. Schuler, and N. D. Spencer, *Biomaterials* 28, 2175 (2007).
21. K. Y. Cai, J. Bossert, and K. D. Jandt, *Colloids Surf. B Biointerfaces* 49, 136 (2006).
22. O. Zinger, G. Zhao, Z. Schwartz, J. Simpson, M. Wieland, D. Landolt, and B. Boyan, *Biomaterials* 26, 1837 (2005).
23. R. A. Gittens, T. McLachlan, R. Olivares-Navarrete, Y. Cai, S. Berner, R. Tannenbaum, Z. Schwartz, K. H. Sandhage, and B. D. Boyan, *Biomaterials* 32, 3395 (2011).

Received: 22 February 2013. Accepted: xx Xxxx xxxx.